

Electronic Supplementary Information

Insights for OCP Identification and Quantification in the Context of Apatite Biomineralization

Marc Robin ^{a,b}, Stanislas Von Euw ^a, Guillaume Renaudin^c, Sandrine Gomes^c,

Jean-Marc Krafft ^b, Nadine Nassif ^a, Thierry Azais ^{a*} and Guylène Costentin ^{b*}

^a Sorbonne Université, CNRS, Collège de France, Laboratoire Chimie de la Matière Condensée de Paris,
LCMCP, F-75005 Paris, France

^b Sorbonne Université, CNRS, Laboratoire Réactivité de Surface, LRS, F-75005 Paris, France

^c Université Clermont Auvergne, CNRS, SIGMA Clermont, ICCF, F-63000 Clermont-Ferrand, France

Corresponding authors: thierry.azais@upmc.fr; guylene.costentin@upmc.fr

S1 Schematic representation of the *in situ* Raman set up

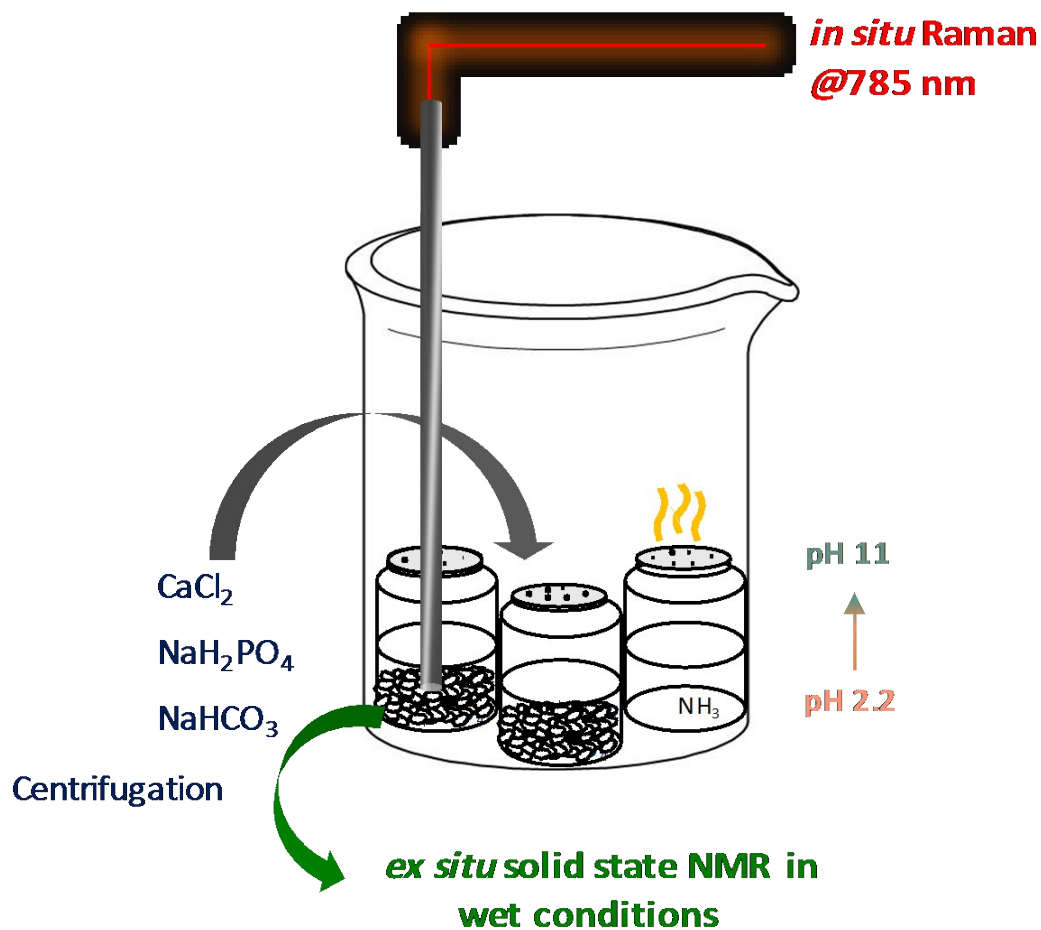


Figure S1. Schematic representation of the original set-up used to monitor the precipitation of biomimetic apatite (cHAp).

S2 decomposition of the Raman spectra from physical mixtures of OCP and cHAp

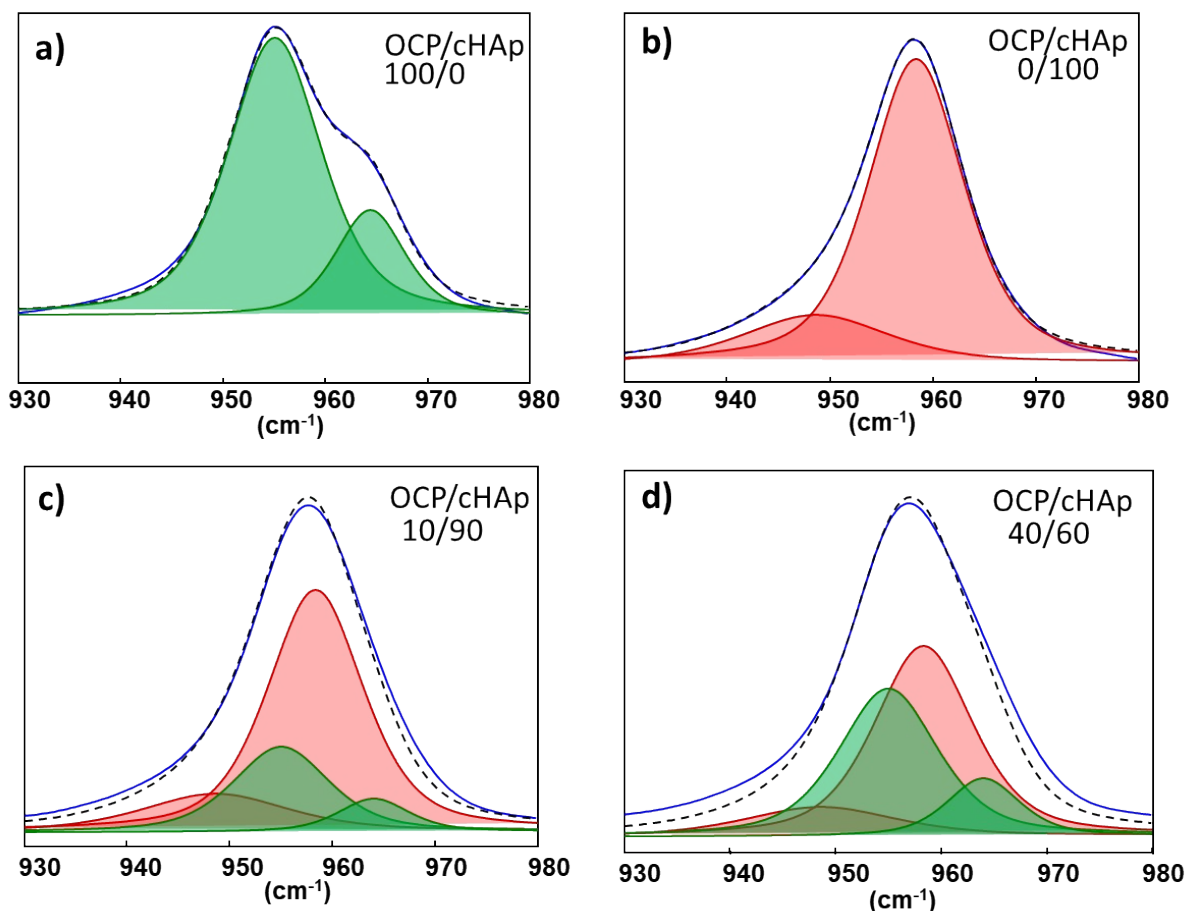
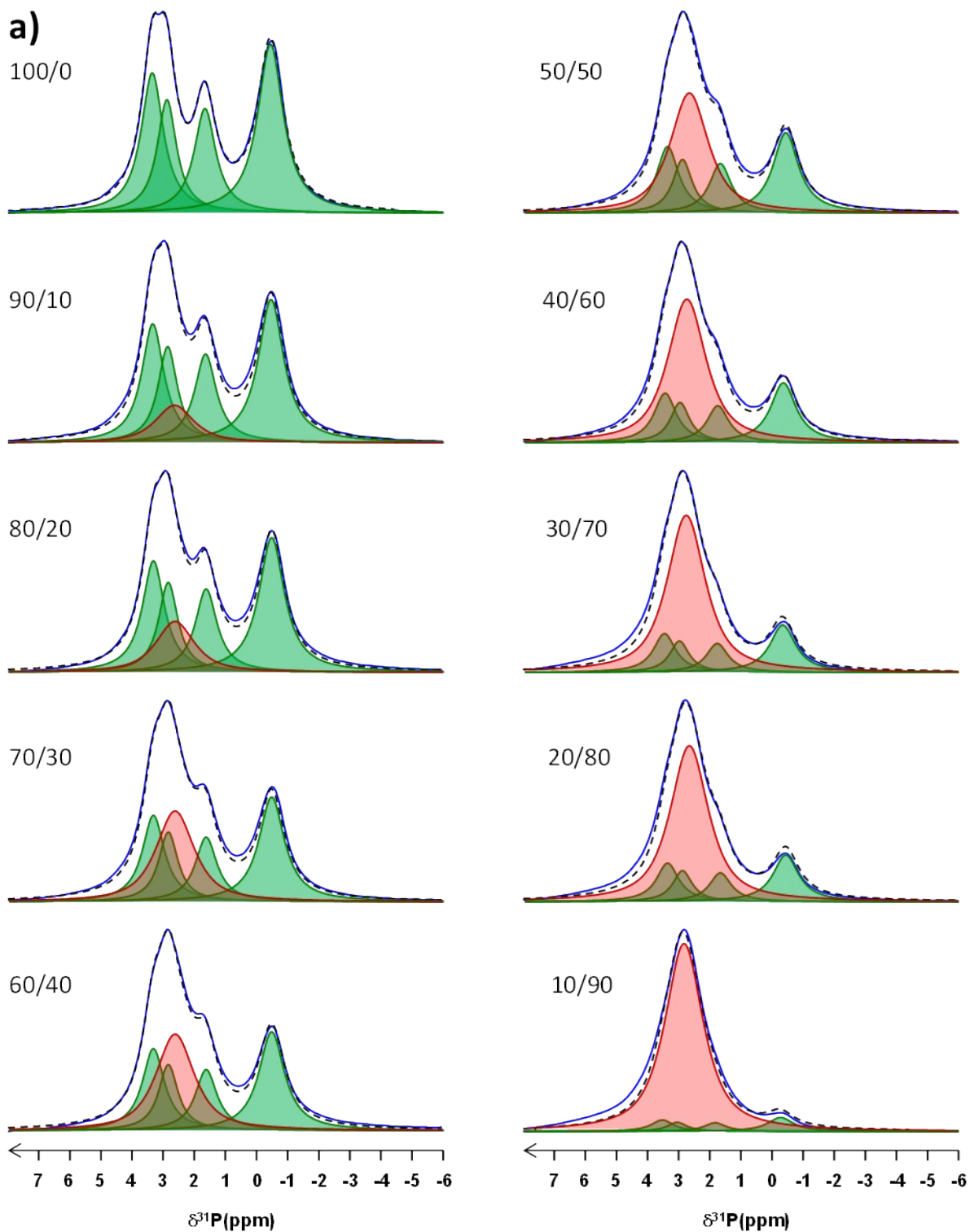
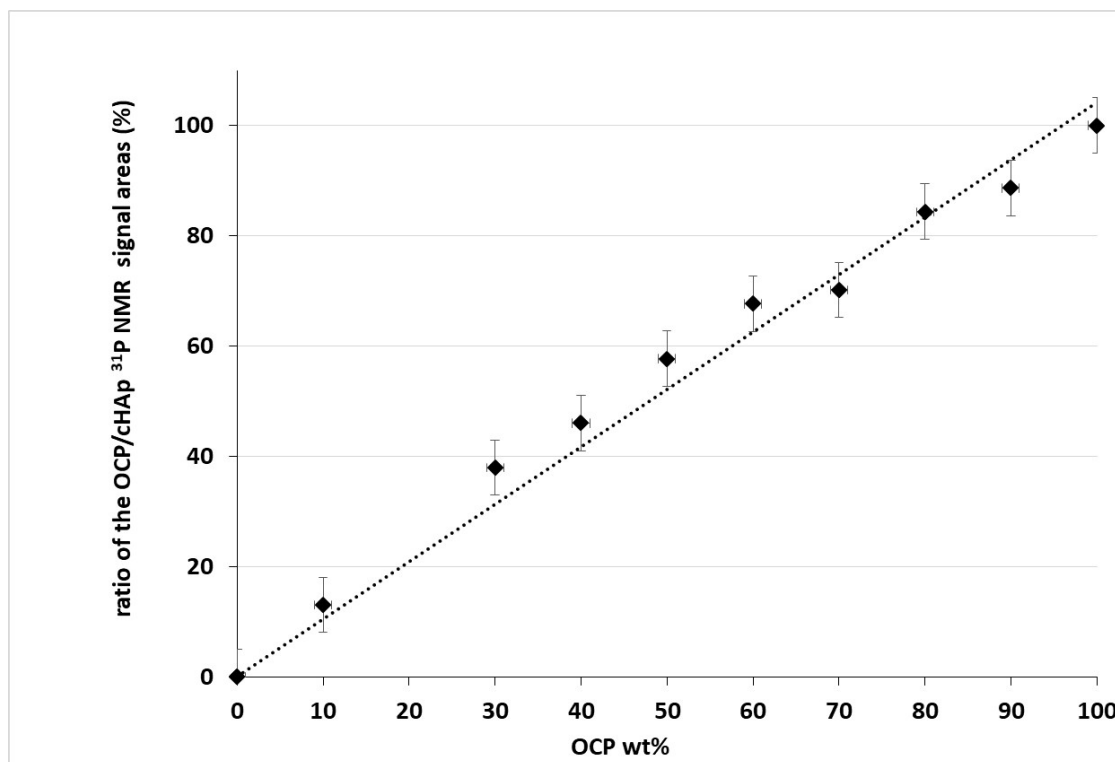


Figure S2. Spectral decomposition Raman spectra in the ν_1 PO_4 region for **a)** pure OCP, **b)** pure cHAp and **c)** and **d)** OCP/cHAp physical mixtures with weight ratio of 10/90 and 40/60, respectively. In these two latter cases, the two set of components extracted for pure OCP and cHAp samples (band positions, linewidths and the relative intensities of the two components present in the pure OCP (955 and 964 cm^{-1}) and cHAp (958 and 950 cm^{-1}) samples were kept constant. The estimated compositions deduced from the extracted contributions of the fits for the two physical mixtures (27/73 and 45/55, respectively) are however not in good accordance with the nominal ones, which is explained by the numerous parameters (surface/volume ratio, diffusion) impacting the intensities of the Raman contributions. Experimental spectrum in blue, ν_1 PO_4 bands related to OCP in green, ν_1 PO_4 bands related to cHAp in red, sum in dashed black.



S3 Decomposition of ^{31}P NMR spectra of physical mixtures of OCP and cHAP and calibration curve.

Figure S3a : decomposition of the ^{31}P ssNMR spectra of the OCP/cHAp physical mixtures. Experimental spectrum in blue, resonances corresponding to OCP in green, to cHAp in red, sum in dashed black. The relative OCP/cHAp nominal weight fraction are indicated onto each spectrum.



b)

Figure S3b : relationship between the wt% OCP in the OCP/cHAp physical mixture and the % of the area of OCP phosphate components as determined through ^{31}P ssNMR to be used as calibration curve for relative quantification. The relative precision that can be estimated about $\pm 5\%$ in our conditions.

S4 Biomimetic apatite precipitation video



Video S4. Video (web enhanced object) of the precipitation of biomimetic apatite in one of the two flasks. The pH is indicated by the changes in the pH indicator colour. Web-Enhanced object is available.

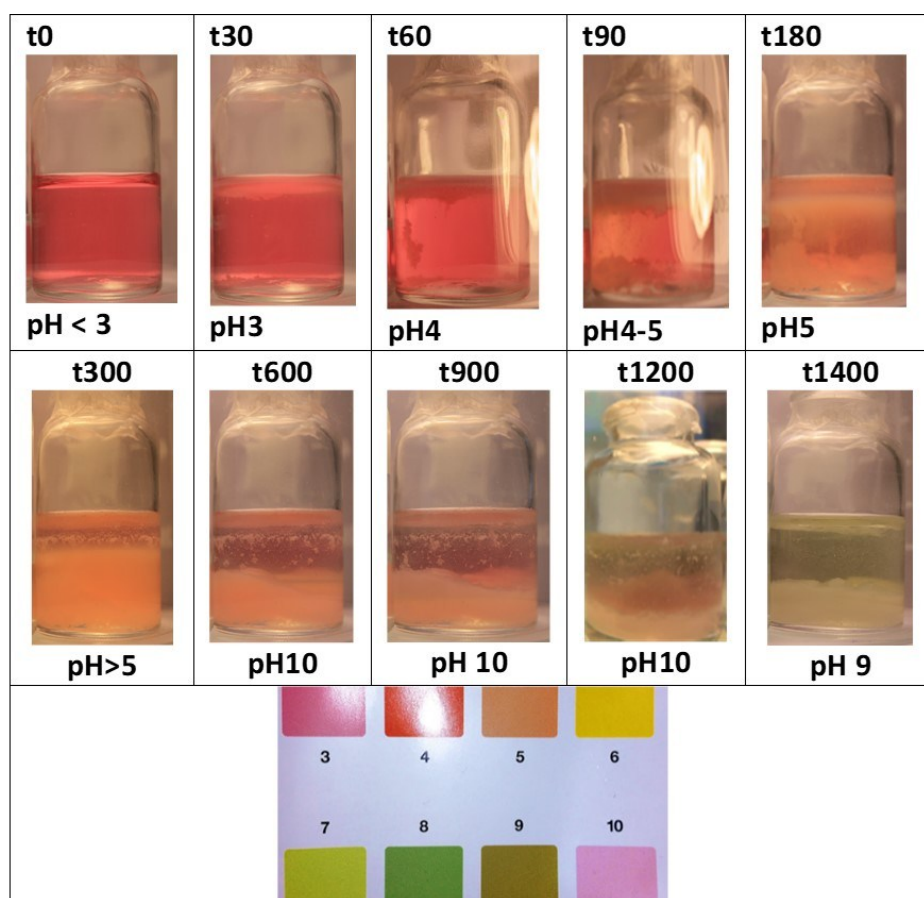


Figure S4. Selection of pictures indicating the evolution of the pH values upon increasing reaction time and corresponding pH value at the bottom of the reactor deduced from universal indicator solution pH (Fluka-31282).

S5 Spectral decomposition of ^{31}P NMR spectra recorded during precipitation of biomimetic apatite

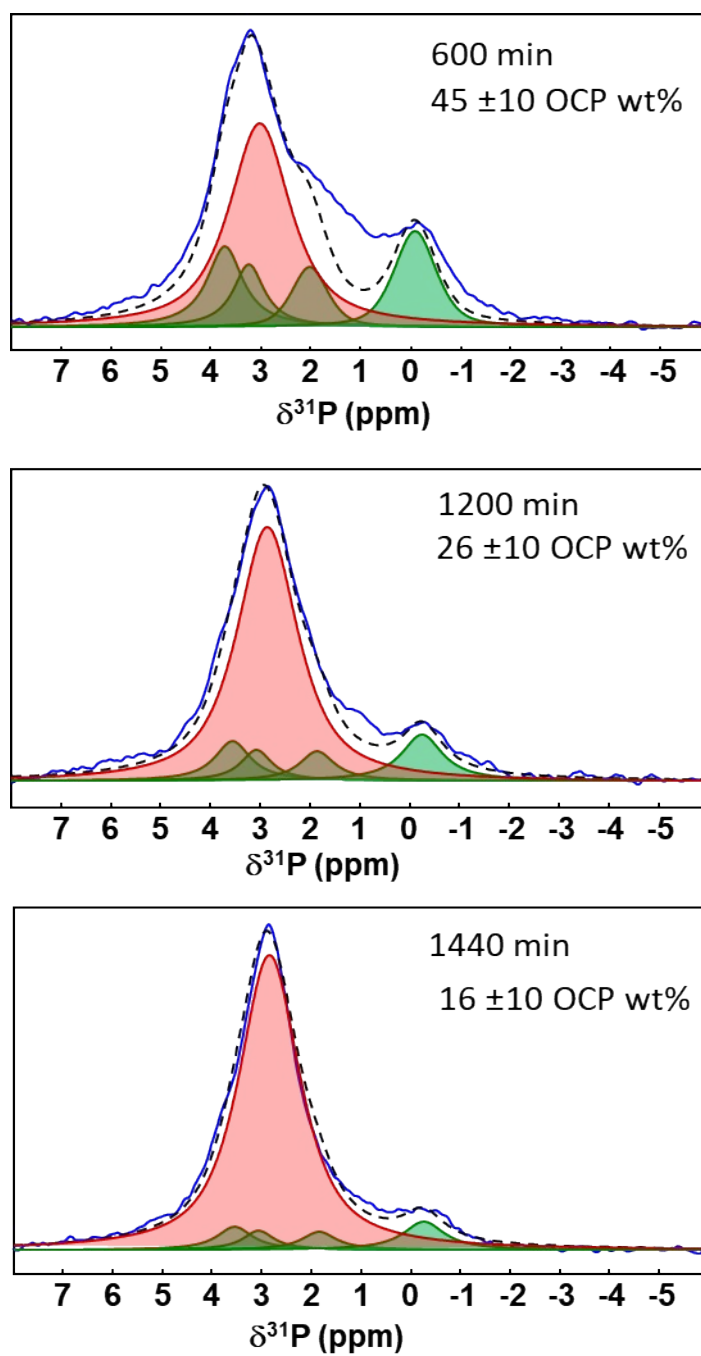


Figure S5: decomposition of the ^{31}P ssNMR spectra of the reaction products during the formation of biomimetic cHAp. Experimental spectrum in blue, resonances corresponding to OCP in green, to cHAp in red, sum in dashed black. The OCP weight fraction that is deduced from the decomposition and the calibration curve (Fig. S3b) is indicated onto each spectrum together with the reaction time.

S6 Rietveld refinement of our OCP sample showing concluding to adequacy with OCP structure model.

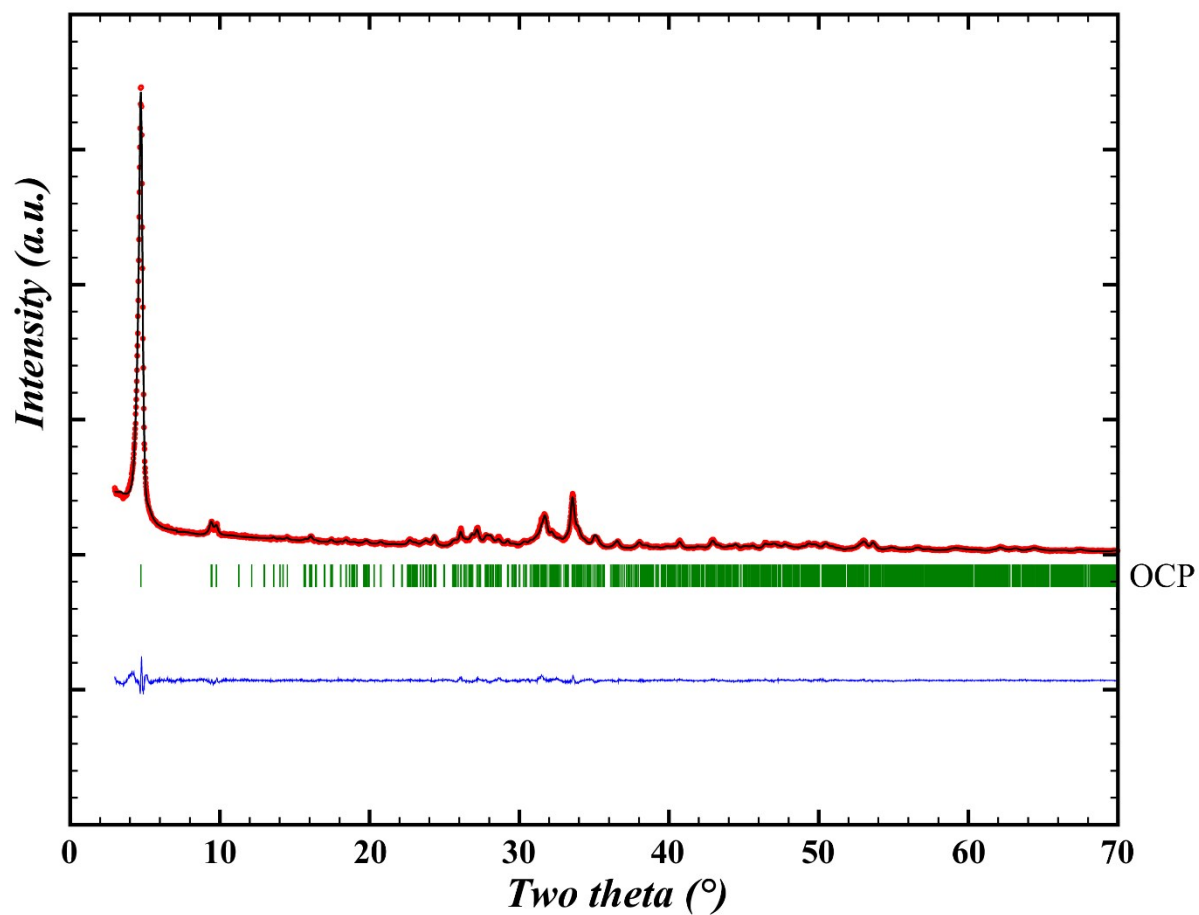


Figure S6. Rietveld plot of our OCP sample showing the adequacy between the OCP model structure and our synthetic single-phase OCP sample ($R_p = 0.05$, $R_{wp} = 0.04$ and $\chi^2 = 2.14$): red point for experimental measurement, black line for calculated pattern, blue line for difference curve and green sticks for OCP Bragg positions ($\lambda = 1.5418 \text{ \AA}$).

Table S6: Structure parameters for OCP compound extracted from Rietveld refinement (standard deviation indicated in bracket) and comparison with values from literature.

		Synthetic OCP	Mathew et al. ¹
OCP cell parameters	a (Å)	19.7084 (6)	19.692 (4)
	b (Å)	9.5405 (5)	9.523 (2)
	c (Å)	6.8367 (3)	6.835 (2)
	α (°)	90.143 (4)	90.15 (2)
	β (°)	92.517 (3)	92.54 (2)
	γ (°)	108.317 (2)	108.65 (1)
	V (Å ³)	1219.00 (9)	1213.1
Rietveld agreement	χ^2	2.14	
factors	Rp (%)	4.05	
	Rwp (%)	5.22	

1 M. Mathew, W. E. Brown, L. W. Schroeder and B. Dickens, *J. Cryst. and Spectrosc.*, 1988, **18**, 235-250

S7 Representation of the OCP structure.

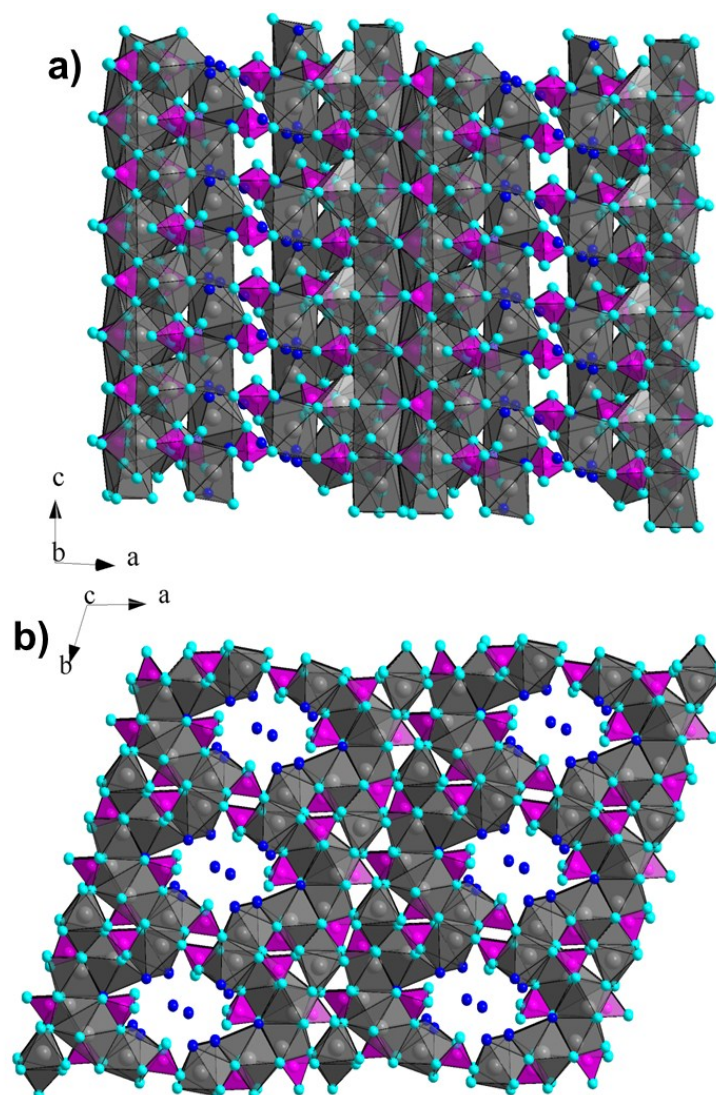


Figure S7: projection of the OCP structure along **a)** the *b* axis and **b)** the *c* axis. Purple tetrahedra correspond to PO_4^{3-} and HPO_4^{2-} , grey polyhedron to coordination spheres of Ca^{2+} , cyan spheres to O^{2-} or OH^- of phosphate groups and blue spheres to water molecules.

S8: Rietveld simulations accounting for the modification of the relative intensity of the (100) diffraction line of OCP.

As shown in Fig. S8, the removal of the water molecule located inside the large column of the OCP unit cell (leading to a theoretical composition of “ $\text{Ca}_8(\text{HPO}_4)_2(\text{PO}_4)_4 \cdot 4\text{H}_2\text{O}$ ”), or the removal of all the water molecules from the hydrated layer (theoretical composition of “ $\text{Ca}_8(\text{HPO}_4)_2(\text{PO}_4)_4 \cdot 0\text{H}_2\text{O}$ ”), lead to the increase of the (100) reflection relative intensity compared to the $(1\bar{1}0)$ and (010) reflections whereas reflexions at high angles (from 20°) are not significantly modified (not shown). On the other hand, increasing of the electronic density within an equivalent of 1 water molecules added inside the large column (theoretical composition of “ $\text{Ca}_8(\text{HPO}_4)_2(\text{PO}_4)_4 \cdot 6\text{H}_2\text{O}$ ”), or formally doubling the electronic density on each water position (theoretical composition of “ $\text{Ca}_8(\text{HPO}_4)_2(\text{PO}_4)_4 \cdot 10\text{H}_2\text{O}$ ”), resulted in the significant decrease of the intensity of the (100) reflexion as observed experimentally for cHAp-1d, cHAp-2d and cHAp-3d samples (Fig. S8).

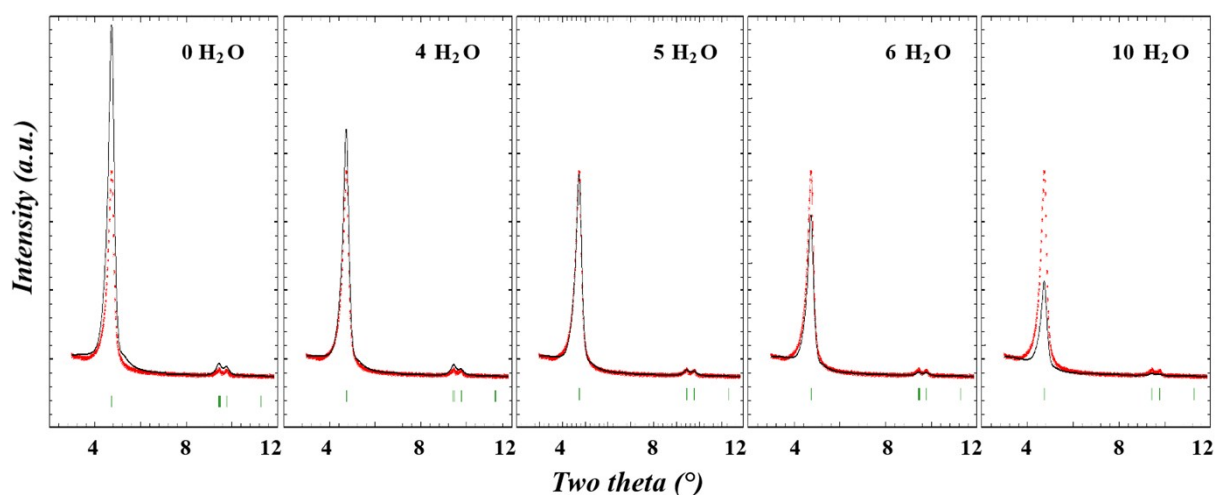


Figure S8: Rietveld simulations displaying the impact of the electronic density expressed as n equivalent of water molecules within the hydrated layer of the OCP structure (i.e. $\text{Ca}_8(\text{HPO}_4)_2(\text{PO}_4)_4 \cdot n\text{H}_2\text{O}$ with $n = 0, 4, 5, 6$ and 10) on the scattered intensity of the first (100) Bragg peak. Red dotted lines and black lines represent the experimental pattern of pure OCP sample and the simulated one with n water molecules respectively.

